Supporting Information

Heterogeneous Acidic TiO_2 Nanoparticles for Efficient Conversion of Biomass Derived Carbohydrates

Chung-Hao Kuo,[a] Altug S. Poyraz,[a] Lei Jin,[a] Yongtao Meng,[a] Lakshitha Pahalagedara,[a] Sheng-Yu Chen,[a] David A. Kriz,[a] Curtis Guild,[a] Anton Gudz,[a] and Steven L. Suib*[a,b]

[a] *Department of Chemistry, University of Connecticut, U-3060, 55 North Eagleville Rd., Storrs, Connecticut 06269 (USA). Fax: +1 860 486 2981; Tel: +1 860 486 2797; E-mail: steven.suib@uconn.edu*
[b] *Institute of Materials Science, University of Connecticut, U-3060, 55 North Eagleville Rd., Storrs, Connecticut 06269 (USA)*

1.1 Detailed methods for catalyst characterization

The catalysts were characterized using several techniques: Powder X-ray diffraction (PXRD) patterns were obtained using a Rigaku UltimaIV X-ray diffractometer with Cu Kα radiation and a beam voltage of 40 kV and 44 mA beam current. Field emission scanning electron microscopy (FESEM) micrographs were taken on a Zeiss DSM 982 Gemini emission scanning microscope with a Schottky Emitter at an accelerating voltage of 2 kV with a beam current of 1 μA. Samples were ultrasonically dispersed in methanol and deposited onto a silicon wafer. High resolution transmission electron microscopy (HRTEM) studies were carried out using a JEOL 2010 transmission electron microscope with an accelerating voltage of 200 kV. The samples were prepared by dispersing the material in methanol. A drop of the dispersion was placed on a carbon coated copper grid and allowed to dry. Thermogravimetric analyses (TGA) were performed on a Hi-Res TA 2950 thermogravimetric analyzer with 60 mL/min of air flow from 25 to 1000 °C at a heating rate of 10 °C/min. Temperature programmed desorption (TPD) was carried

out in a furnace with a quadrupole MS residual gas analyzer. Catalyst powder (200 mg) was placed in a quartz tube and then pretreated in helium flow (100 mL/min) at 180 °C for 1 h to dry the catalyst. After the pretreatment, 10 % NH_3 in Ar (100 mL/min) was fed at room temperature for 1 h, followed by feeding pure helium flow (100 mL/min) for another 2 h to remove the physically adsorbed NH_3. The acid sites of the catalyst were analyzed by following the m/z = 17 signal over a temperature range from room temperature to 800 °C in pure helium flow (100 mL/min). The m/z = 64 signal was also followed to check the decomposition of sulfate ion to SO_2 gas. FT-IR spectra were recorded using a Thermo Scientific Nicolet 8700 spectrometer. The samples were pressed into pellets and self-supporting wafers in a holder in an *in situ* cell and dried at 200 °C for 12 hours before analysis. To obtain the spectra of pyridine adsorbed on the surface, the samples were exposed to pyridine vapor for 1 hour at room temperature. Spectra were then recorded after evacuation (10^{-2} Torr) for 30 min at 200 °C. The Brunauer-Emmett-Teller (BET) surface area of TiO_2 was measured using a Quantachrome Autosorb-1-C automated N_2 gas adsorption system. Samples (150 mg) were pre-degassed at 150 °C for about 12 hours to remove water and other physically adsorbed species. The N_2 isothermal adsorption and desorption experiments were performed at relative pressures (P/P_0) from 10^{-3} to 0.992 and from 0.992 to 0.01, respectively. The thermogravimetric titration analysis was done using

2,6- and 3,5- lutidine as probing bases. The acid amount of the solid acids was calculated by subtracting the weight loss for the desorption of base from the materials.

1.2 Analysis of carbohydrate conversion reaction

The undiluted reaction mixture was characterized using a gas chromatograph (HP 5890 series II) equipped with a DB-17MS capillary column (20.0 m x 180 μm x 0.18 μm) and mass selective detector (5971 series). The reaction mixture was also analyzed with a Shimadzu series HPLC (Biorad Aminex HPX-87H column) with an RI detector using 0.005 M H_2SO_4 (rate = 0.6 mL/min) as eluents. An HP 5890 series II GC system equipped with a MTX®-biodiesel TG w/Integra-GapTM capillary column (14.0 m x 530 μm x 0.16 μm) and an FID detector was used for quantitative analysis. The yields of organic products were obtained from GC analyses based on a calibration curve from commercial or synthesized samples and an internal standard (1-octanol). The yields were calculated on a carbon-basis. Carbohydrate conversions were determined from HPLC data. The conversion was calculated from the fructose, glucose, sucrose, and cellobiose on a carbon-basis. The polysaccharide conversions of cellulose and starch were further calculated by subtracting the weight of remaining solids (unreacted biomass) at the end of the reaction. The data were obtained using the following equations:

Monosaccharides conversion (%) = 100(A-C)／A

Polysaccharides conversion (%) = 100(B-C-D)／B

Organic products yield (%) = 100E／A or B

A: total amount (mol) of monosaccharides used.

B: total amount (mol) of glucose monomer in cellulose.

C: total amount (mol) of remaining monosaccharides.

D: the unreacted biomass after reaction.

E: total amount (mol) of organic products produced by catalytic reaction.

2. Disscussion of catalyst characterization

PXRD, FESEM, HRTEM and N_2 sorption analyses. As-Synthesized TiO_2 nanoparticles were indicated as the anatase phase in PXRD analysis (see ESI†, Fig. S6). The broadening of diffraction lines indicates small crystallite sizes. Crystallite sizes were calculated to be an average of ~ 4 nm using Scherrer's equation. The anatase phase was maintained up to 800 °C and fully converted to the rutile phase by 1000 °C. The FESEM images show mostly micron size aggregated powder and with no distinct particle morphology. The HRTEM images confirmed the nano-size nature of synthesized TiO_2 particles. The HRTEM image shows that the powder sample consists of aggregated nanoparticles and estimated particles size were consistent with

XRD data (~ 4 nm) (see ESI†, Fig. S7). The BET surface area of the TiO_2 was calculated to be 238 m^2 g^{-1} from N_2 sorption data, which is high compared to other tested catalysts.

Pyridine-adsorption and FT-IR experiments. The type of acid sites on TiO_2 nanoparticles was determined by pyridine adsorption and FT-IR spectroscopy (see ESI†, Fig. S8, 9). The FT-IR spectrum of TiO_2 nanoparticles without pyridine adsorption treatment showed the typical surface SO_4^{2-} stretch modes in the 1000-1500 cm^{-1} region. The vibrations at 1045 cm^{-1}, 1132 cm^{-1} and 1221 cm^{-1} are attributed to surface SO_3^- stretches. The band at 1400 cm^{-1} is ascribed to O=S=O stretching of SO_4^{2-} groups, which could be chelating in bidentate or bridged bidentate forms on the surface of the TiO_2 nanoparticles.[1] In the pyridine-adsorption FT-IR spectrum, three peaks were observed in the region between 1400 ~ 1600 cm^{-1} due to C–C stretching vibrations of pyridine. The peak at 1445 cm^{-1} was assigned to pyridine adsorbed on Lewis acid sites; the peak at 1548 cm^{-1} is characteristic of pyridine adsorbed on Brønsted acid sites and the peak at 1490 cm^{-1} appears for pyridine adsorbed on both Brønsted and Lewis acid sites.[1]

NH_3-TPD and TGA analyses. NH_3-TPD experiments were conducted to determine the relative strengths of acid sites (see ESI†, Fig. S10). A major desorption occurred between 150 to 500 °C, and another minor desorption peak between 550 to

700 °C. The desorption peak centered at ~ 325 °C is attributed to NH_3 adsorbed on weak acid sites while the one centered at ~ 600 °C is due to NH_3 adsorbed on strong acid sites.[2] The amount of SO_4^{2-} ions attached to the surface of the TiO_2 nanoparticles was determined by TGA experiments (see ESI†, Fig. S11). A 3 % mass decrease was observed between 450 and 700 °C, which resulted from decomposition of SO_4^{2-} ions from the TiO_2 surface. This is also shown by the TPD experiments where SO_2 (decomposition of SO_4^{2-} ions, m/z = 64) was detected starting at 450 °C. These data suggest that the weight loss peak around 600 °C can properly be ascribed to SO_4^{2-} ions decomposition.

3. The synthesis and characterizations procedures of standard chemicals levulinic esters and HMF-derived ethers

^1H and ^{13}C NMR spectra were recorded on a Bruker AVANCE III- 400 MHz spectrometer. ^1H NMR spectra were collected at 400 MHz with chemical shift referenced to the residual peak in $CDCl_3$ (δ: H 7.26 ppm). ^{13}C NMR spectra were collected at 100 MHz and referenced to residual peak in $CDCl_3$ (δ: C 77.0 ppm) or CD_3OD (δ: C 49.1 ppm). Multiplicities are given as s (singlet), d (doublet), t (triplet), and m (multiplet).

3.1 Preparation and characterization of levulinic esters

***n*-Propyl levulinate** To a mixture of levulinic acid (5.8 g, 0.05 mol), and *n*-propanol (7.5 g, 0.125 mol) in toluene (15 mL) was added H_2SO_4 (0.1 mL) dropwise under reflux. The mixture was refluxed for 4 h. After cooling, the reaction mixture was added to dichloromethane and washed with H_2O. The organic layer was dried over $MgSO_4$. After removal of the solvent, the residue was purified by vacuum distillation to yield *n*-propyl levulinate as a colorless liquid. ^{1}H NMR ($CDCl_3$, 400 MHz): δ: 4.04 ~ 4.00 (m, 2H), 2.74 (t, J = 6.6 Hz, 2H), 2.57 (t, J = 6.6 Hz, 2H), 2.18 (s, 3H), 1.68 ~ 1.59 (m, 2H), 0.93 (t, J = 7.4 Hz, 3H). ^{13}C NMR ($CDCl_3$, 100 MHz): δ: 206.6, 172.8, 66.2, 37.9, 29.8, 28.0, 21.9, 10.3. HRMS *m/z* $(M + H)^+$ for $C_8H_{15}O_3$ 159.1021, found 159.0993.

2-Propyl levulinate 2-Propyl levulinate was obtained from 2-propanol as a colorless liquid following the procedure for the preparation of *n*-propyl levulinate. ^{1}H NMR ($CDCl_3$, 400 MHz): δ: 5.01 ~ 4.95 (m, 1H), 2.72 (t, J = 6.6 Hz, 2H), 2.53 (t, J = 6.6 Hz, 2H), 2.17 (s, 3H), 1.22 (s, 3H), 1.21 (s, 3H). ^{13}C NMR ($CDCl_3$, 100 MHz): δ: 206.7, 172.2, 67.9, 38.0, 29.8, 28.4, 21.7 (2C). HRMS *m/z* $(M + H)^+$ for $C_8H_{15}O_3$ 159.1021, found 159.0995.

2-Butyl levulinate 2-Butyl levulinate was obtained from 2-butanol as a colorless liquid following the procedure for the preparation of *n*-propyl levulinate. ^{1}H NMR ($CDCl_3$, 400 MHz): δ: 4.86 ~ 4.78 (m, 1H), 2.73 (t, J = 6.6 Hz, 2H), 2.53 (t, J = 6.6

Hz, 2H), 2.18 (s, 3H), 1.62 ~ 1.48 (m, 2H), 1.18 (d, J = 6.3 Hz, 3H), 0.88 (t, J = 7.4 Hz, 3H). ^{13}C NMR ($CDCl_3$, 100 MHz): δ: 206.7, 172.4, 72.5, 38.0, 29.8, 28.7, 28.3, 19.4, 9.6 HRMS *m/z* $(M + H)^+$ for $C_9H_{17}O_3$ 173.1178, found 173.1162.

***t*-Butyl levulinate** To a mixture of levulinic acid (5.9 g, 0.05 mol), and *t*-butanol (7.6 g, 0.1 mol) in dichloromethane (80 mL) was added 4-dimethylaminopyridine (DMAP) (1.8 g, 0.015 mol) under r.t. Then, N,N'-dicyclohexylcarbodiimide (DCC) (12.5 g, 0.06 mol) was added at 0 °C. After stirring at r.t. for 10 h, the urea was filtered and the organic layer was concentrated in vacuum. After removal of the solvent, the residue was purified by vacuum distillation to yield *t*-butyl levulinate as a colorless liquid. ^{1}H NMR ($CDCl_3$, 400 MHz): δ: 2.68 (t, J = 6.6 Hz, 2H), 2.48 (t, J = 6.6 Hz, 2H), 2.17 (s, 3H), 1.43 (s, 9H). ^{13}C NMR ($CDCl_3$, 100 MHz): δ: 206.9, 172.0, 80.6, 38.1, 29.9, 29.2, 28.0 (3C). HRMS *m/z* $(M + H)^+$ for $C_9H_{17}O_3$ 173.1178, found 173.1188.

3.2 Preparation and characterization of hydroxymethylfurfural ethers

5-(Isopropoxymethyl)furan-2-carbaldehyde A mixture of hydroxymethylfurfural (0.3 g, 2.38 mmol) and TiO_2 nanoparticles (100 mg) in 2-propanol (6 mL) was heated to 100 °C for 6 h. After cooling, the reaction mixture was added to dichloromethane and washed with H_2O. The organic layer was dried over $MgSO_4$. After removal of the solvent, the residue was purified by column chromatography

(dichloromethane/hexane=1/1) to yield 5-(isopropoxymethyl)furan-2-carbaldehyde as a light yellow liquid. ^{1}H NMR ($CDCl_3$, 400 MHz): δ: 9.59 (s, 1H), 7.19 (d, J = 3.5 Hz, 2H), 6.50 (d, J = 3.5 Hz, 2H), 4.52 (s, 2H), 3.74 ~ 3.64 (m, 1H), 1.20 (s, 3H), 1.19 (s, 3H). ^{13}C NMR ($CDCl_3$, 100 MHz): δ: 177.6, 159.4, 152.4, 122.1, 110.7, 72.1, 62.5, 21.9 (2C). HRMS *m/z* $(M + H)^+$ for $C_9H_{13}O_3$ 169.0865, found 169.0852.

5-(*sec*-Butoxymethyl)furan-2-carbaldehyde

5-(*sec*-Butoxymethyl)furan-2-carbaldehyde was obtained from 2-butanol as a mixture of diastereomers (6:1) a light yellow liquid following the procedure for the preparation of 5-(isopropoxymethyl)furan-2-carbaldehyde. ^{1}H NMR ($CDCl_3$, 400 MHz): δ: δ: 9.60 (s, 1H), 7.20 ~ 7.19 (m, 2H), 6.50 (d, J = 3.5 Hz, 2H), 4.59 ~ 4.48 (m, 2H), 3.51 ~ 3.43 (m, 1H), 1.64 ~ 1.52 (m, 2H), 1.17 ~ 1.16 (m, 3H), 0.92 ~ 0.88 (m, 3H). ^{13}C NMR (CD_3OD, 100 MHz): δ: 179.5, 161.0, 154.0, 124.5, 112.3, 78.5, 63.6, 30.3, 19.5, 10.1. HRMS *m/z* $(M + H)^+$ for $C_{10}H_{15}O_3$ 183.1021, found 183.1002.

The ^{1}H and ^{13}C NMR of 5-(*sec*-butoxymethyl)furan-2-carbaldehyde contained signals that we ascribed to the diastereomer, which accounted for approximately 15% of product material. Selected ^{1}H signals of the minor isomer: 9.63 (s, 0.15H), 6.62 (d, J=8.7 Hz, 0.15H), 5.60 (t, J=5.8 Hz, 0.15H), 5.29 (s, 0.15 H), 3.76 ~ 3.70 (m, 0.15H). Selected ^{13}C signals of the minor isomer: 63.48, 19.48, 10.03.

5-(*tert*-Butoxymethyl)furan-2-carbaldehyde

5-(*tert*-Butoxymethyl)furan-2-carbaldehyde was obtained from *t*-butanol as a light yellow liquid following the procedure for the preparation of 5-(isopropoxymethyl)furan-2-carbaldehyde. ^{1}H NMR ($CDCl_3$, 400 MHz): δ: 9.54 (s, 1H), 7.16 (d, J = 3.5 Hz, 2H), 6.45 (d, J = 3.5 Hz, 2H), 4.43 (s, 2H), 1.22 (s, 9H). ^{13}C NMR ($CDCl_3$, 100 MHz): δ: 177.4, 160.1, 152.2, 122.3, 110.2, 74.3, 57.1, 27.3 (3C). HRMS *m/z* $(M + H)^+$ for $C_{10}H_{15}O_3$ 183.1021, found 183.1035.

Reference:

1. a) J. R. Sohn and D. C. Shin, *Appl. Catal. B*, 2008, **77**, 386-394; b) H. Nakabayashi, *Bull. Chem. Soc. Jpn.*, 1992, **65**, 914.

2. K. Okumura, T. Tomiyama, S. Shirakawa, S. Ishida, T. Sanada, M. Arao and M. Niwa, *J. Mater. Chem.*, 2011, **21**, 229.

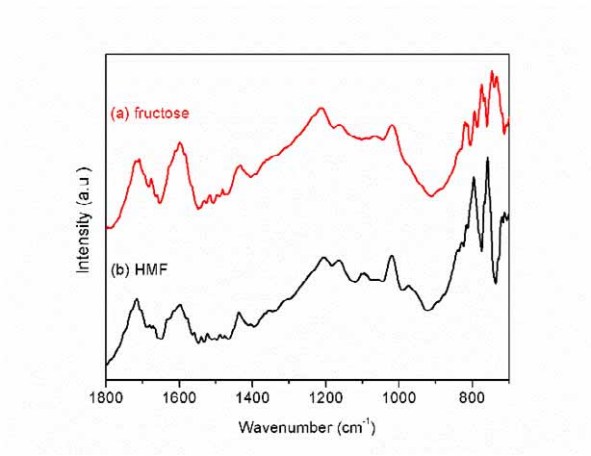

Fig. S1 IR spectra of (a) humins formed using HMF as substrate, and (b) humins formed using fructose as substrate.

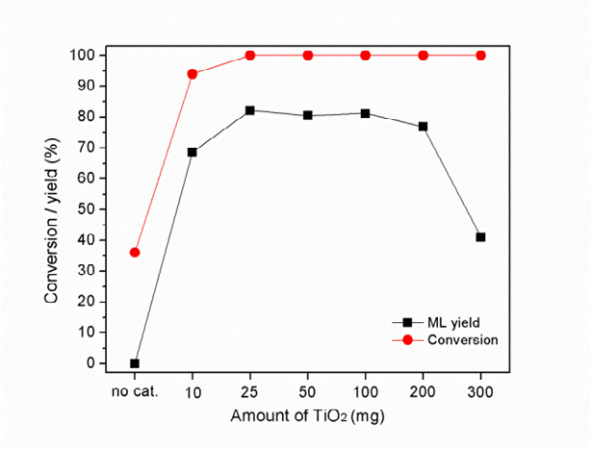

Fig. S2 Effect of catalyst loading on conversion of fructose to ML. (*Reaction conditions*: 0.05 M fructose in MeOH, 175 ^{o}C, 1 h.)

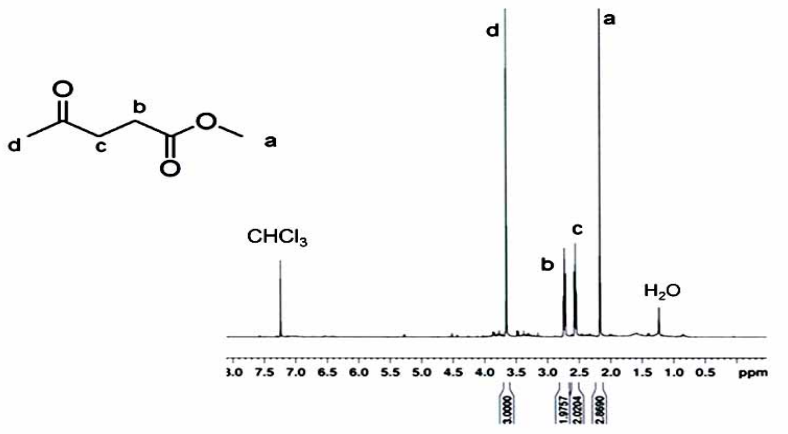

Fig. S3 The NMR spectrum of product after the TiO_2 nanoparticles catalyzed reaction.

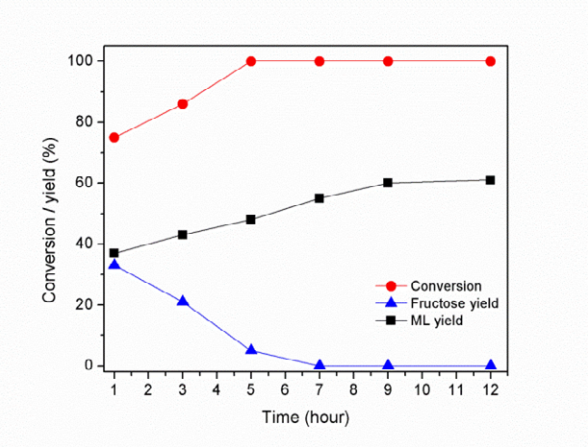

Fig. S4 Effect of time on conversion of glucose to fructose and ML. (*Reaction conditions*: 0.18 g glucose in 20 mL MeOH, 0.1 g catalyst, 175 ^{o}C.)

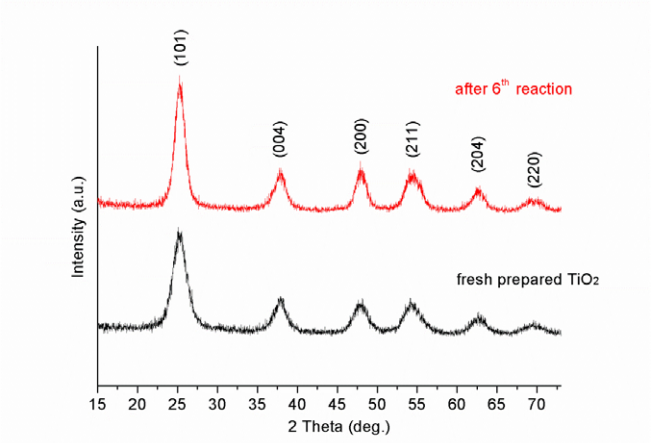

Fig. S5 The X-ray diffractograms of the freshly prepared TiO_2 and after the 6th use.

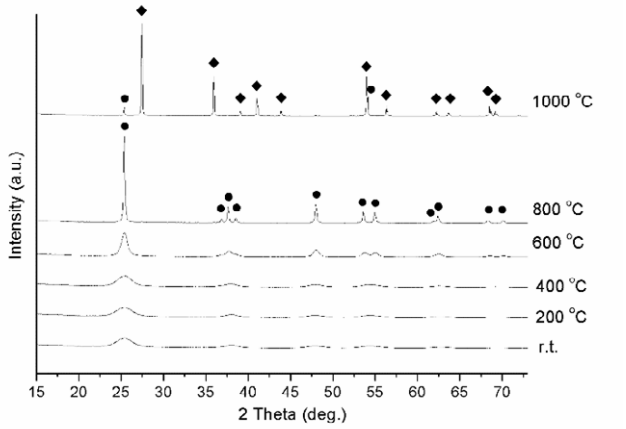

Fig. S6 The X-ray diffractograms of synthesized TiO_2 at various temperatures. (●: anatase phase, ◆: rutile phase.)

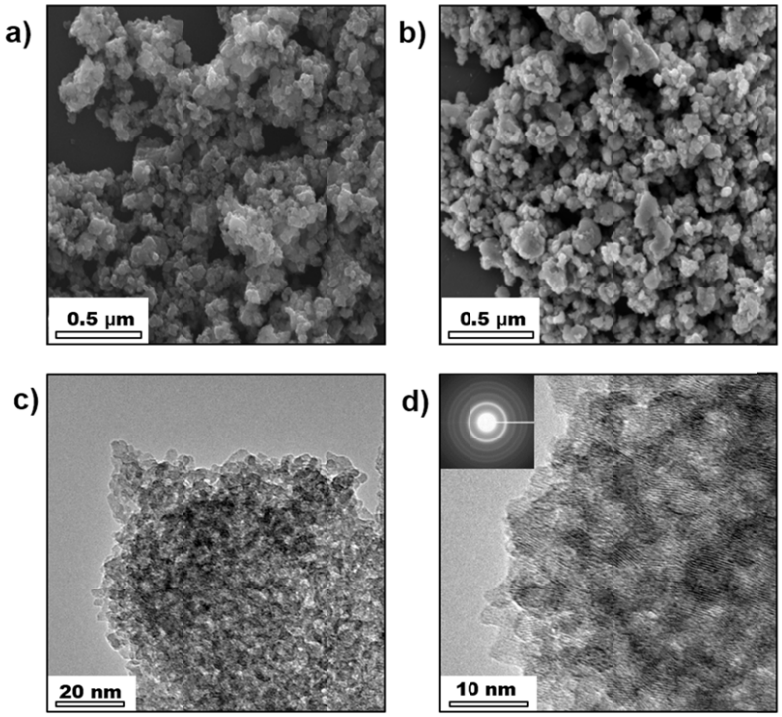

Fig. S7 The SEM and TEM images of TiO_2 nanoparticles (a) SEM image of freshly prepared TiO_2; (b) SEM image of after the 6th reaction; (c,d) TEM images of freshly prepared TiO_2. Inset: SAED of freshly prepared TiO_2 nanoparticles.

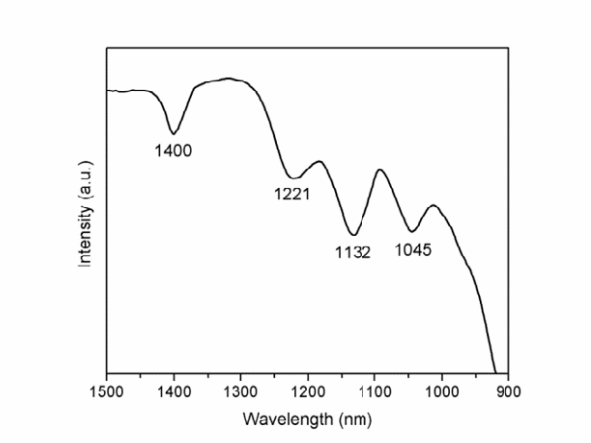

Fig. S8 The IR spectrum of freshly prepared TiO_2 nanoparticles.

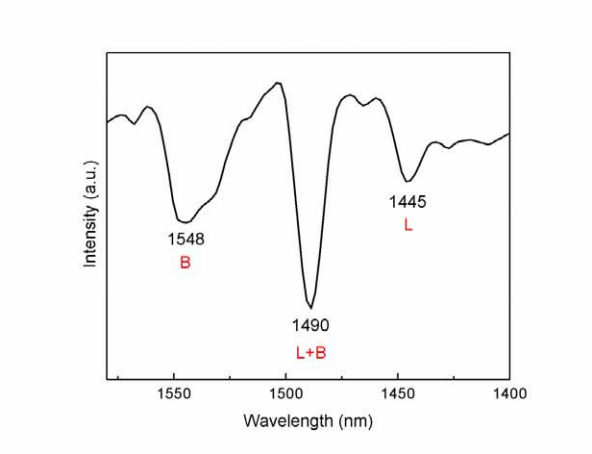

Fig. S9 The pyridine adsorption IR spectrum of TiO_2 nanoparticles.

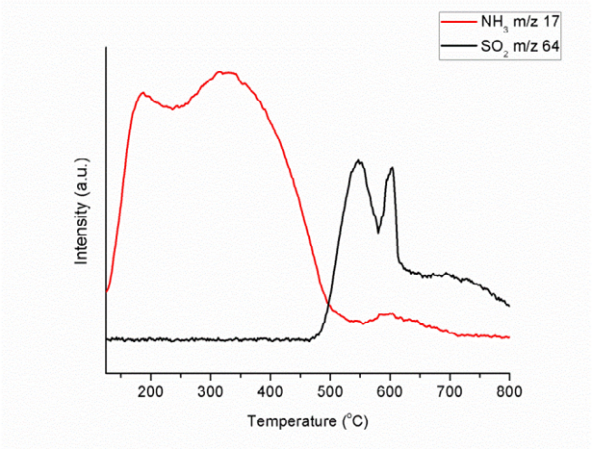

Fig. S10 The NH_3-TPD desorption analysis of freshly prepared TiO_2 nanoparticles.

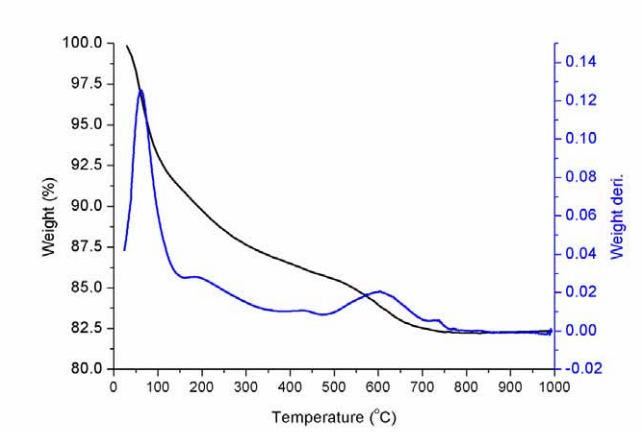

Fig. S11 The TGA data for freshly prepared TiO_2 nanoparticles.

Table S1. The carbon balance calculation of biomass derived carbohydrates conversion using TiO_2 nanoparticles.

Products	Fructose	Glucose	Sucrose	Cellobiose	Cellulose	Starch
Methyl levulinate	58%	44%	47%	42%	30%	29%
Methyl formate	20%	10%	9%	7%	4%	3%
Unconverted sugars	n.d.	<1%	<1%	<1%	-[a]	-[a]
HMF & furfural derivatives	<1%	<1%	<1%	<1%	1%	3%
Unidentified compounds	4%	10%	13%	11%	10%	15%
Humins on the glassware wall	3%	6%	4%	5%	9%	7%
Humins on the catalyst	1.5%	1.5%	1.5%	2%	2%	2%
Residuals remained	3.5%	4.5%	5%	4%	28%	33%
Unaccounted	9%	22%	18.5%	27%	16%	8%
Carbon balance	91%	78%	81.5%	73%	84%	92%

[a] The unconverted sugars of cellulose and starch were combined with residuals remained

Table S2. The analysis of the concentration of SO_4^{2-} on the surface of TiO_2

Treatment	S (Wt%) XPS	S (Wt%) EDAX	S (Wt%) TGA	ML yield %
r.t.	2.4	2.6	3.1	79
200 °C	2.5	2.7	3.0	81
400 °C	2.1	2.4	2.8	83
600 °C	1.0	1.3	1.4	83
800 °C	0	0.3	0.1	2
TiO_2 after 6^{th} run	1.6	2.0	2.5	69

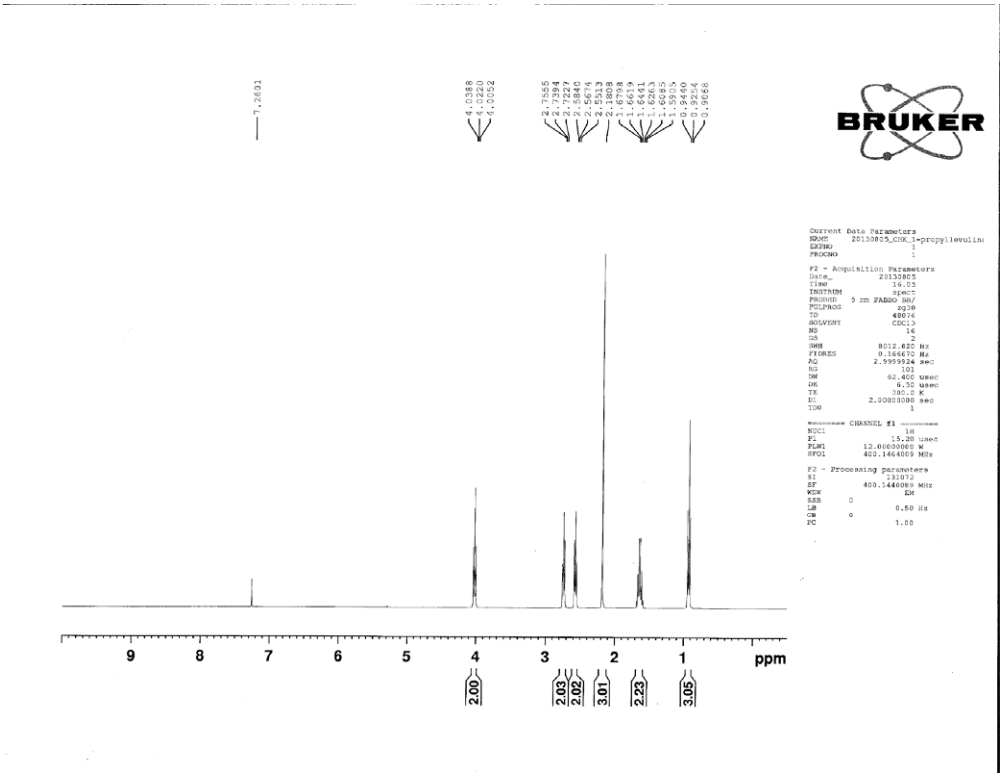

The ^{1}H spectrum of *n*-propyl levulinate

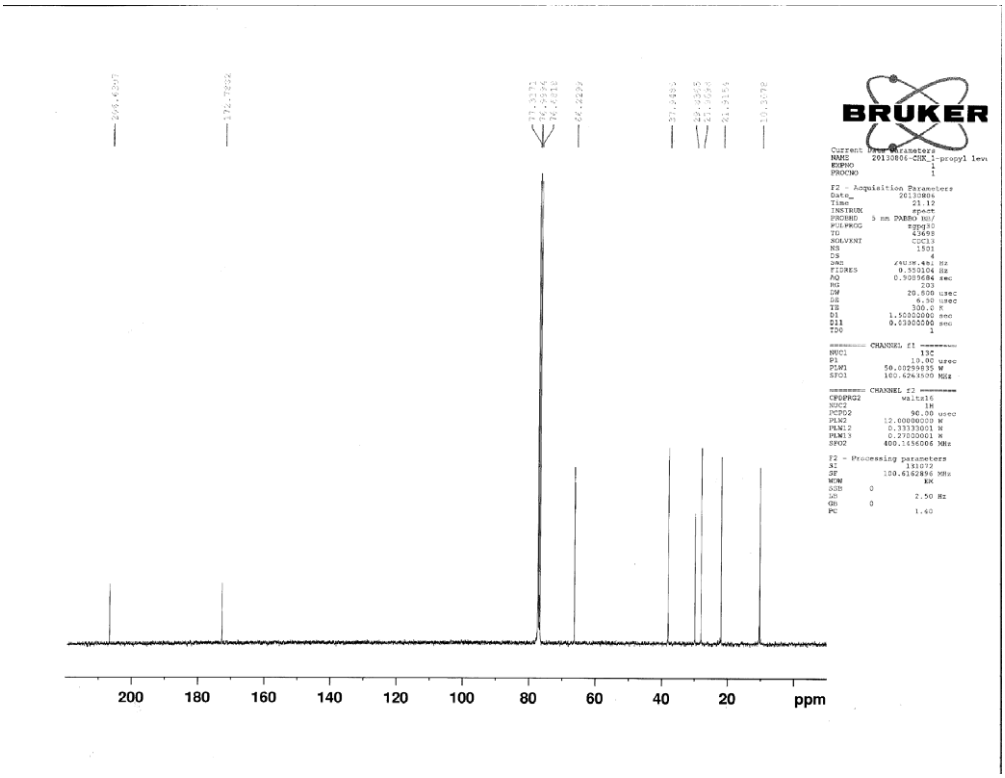

The ^{13}C spectrum of *n*-propyl levulinate

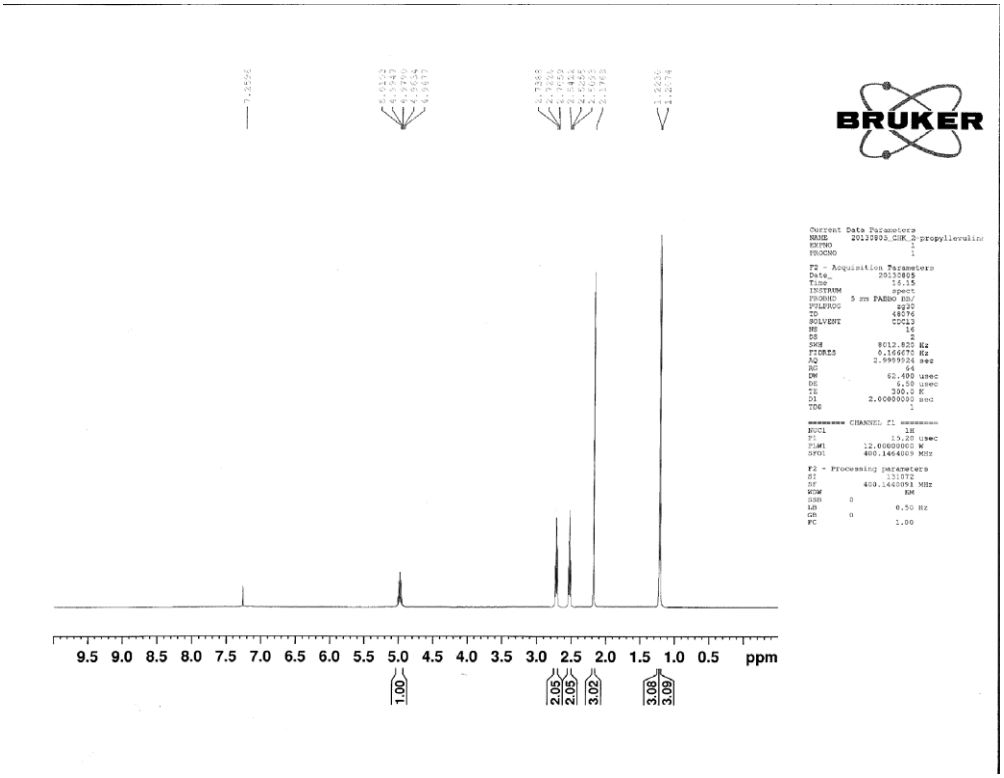

The ^{1}H spectrum of 2-propyl levulinate

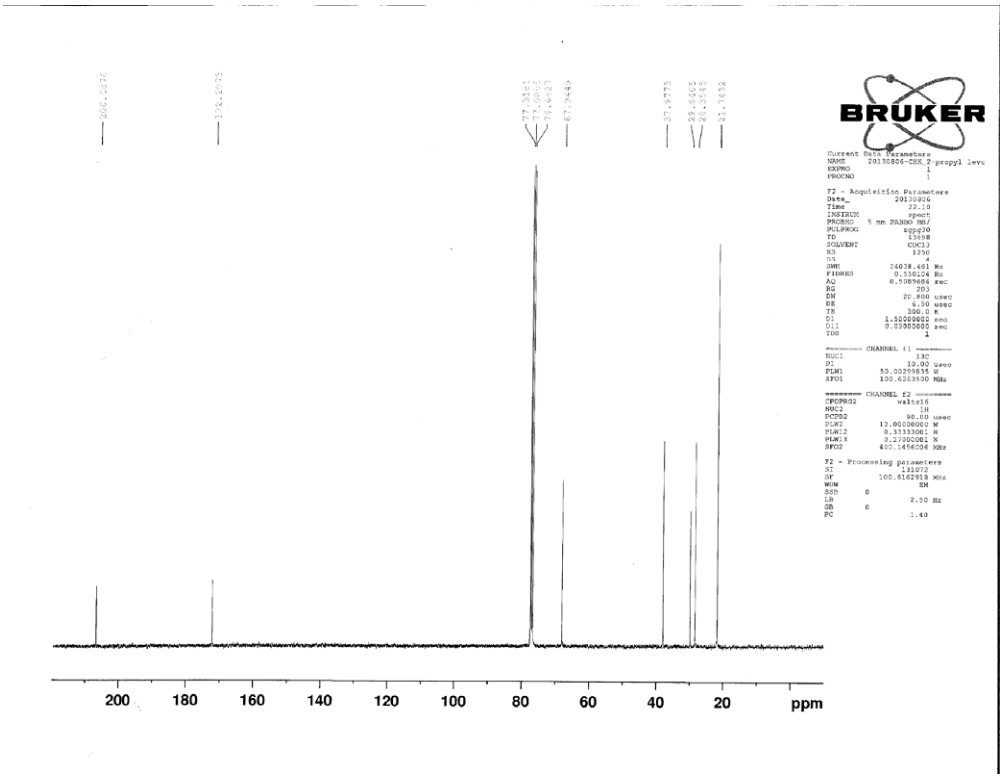

The ^{13}C spectrum of 2-propyl levulinate

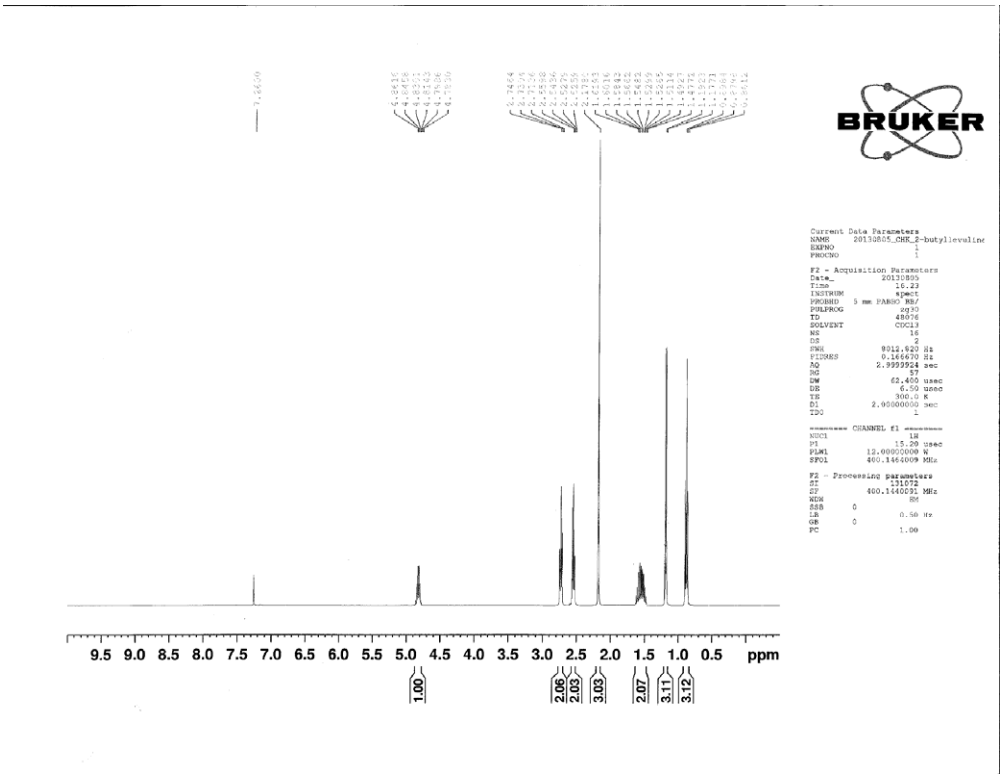

The ^{1}H spectrum of 2-butyl levulinate

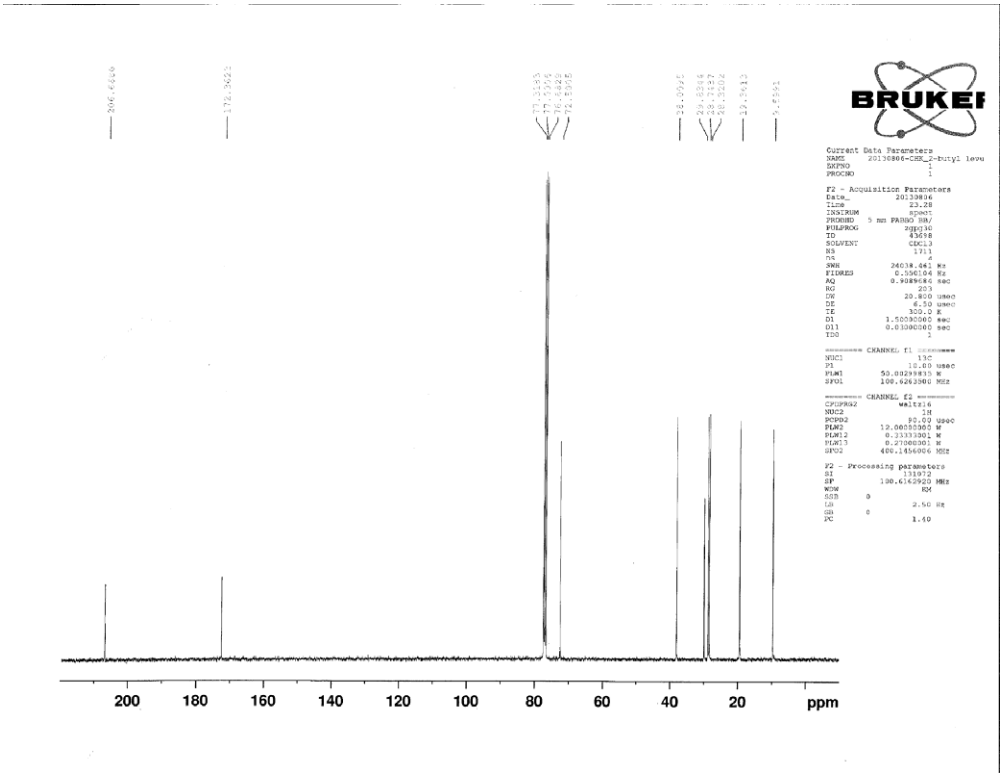

The ^{13}C spectrum of 2-butyl levulinate

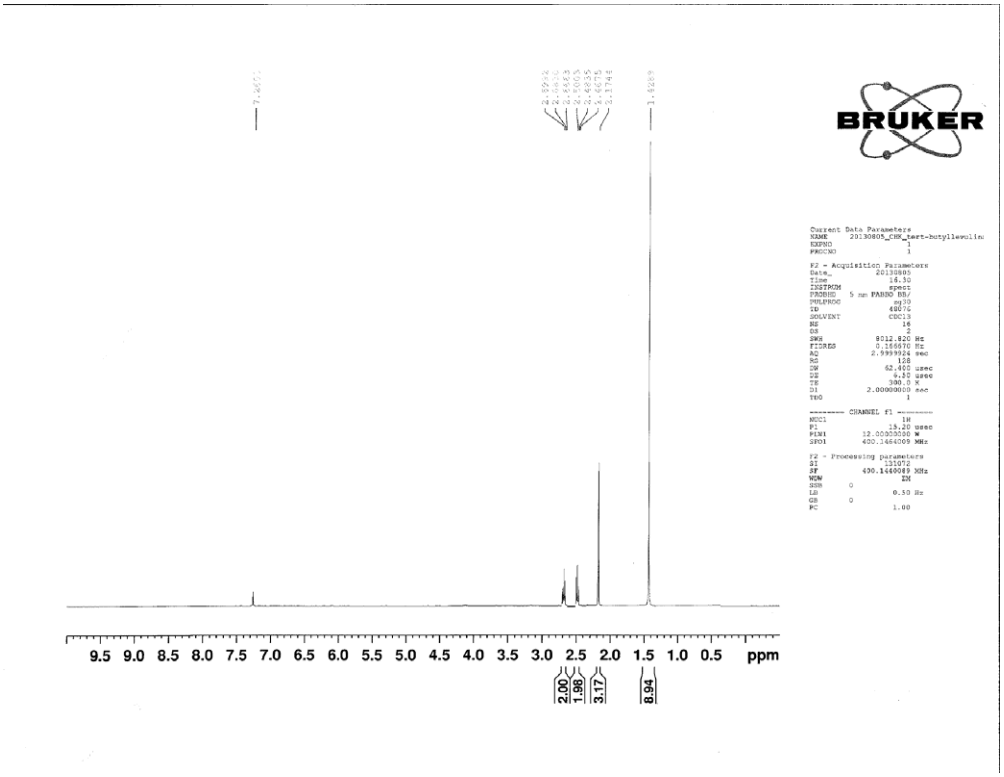

The ^{1}H spectrum of *t*-butyl levulinate

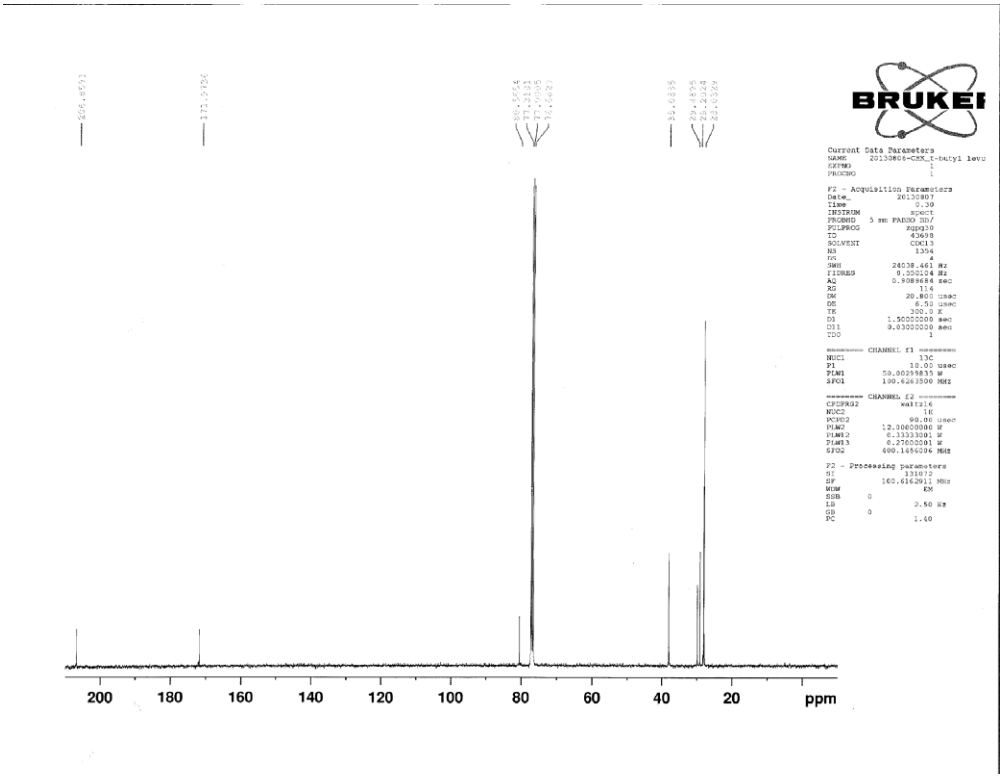

The ^{13}C spectrum of *t*-butyl levulinate

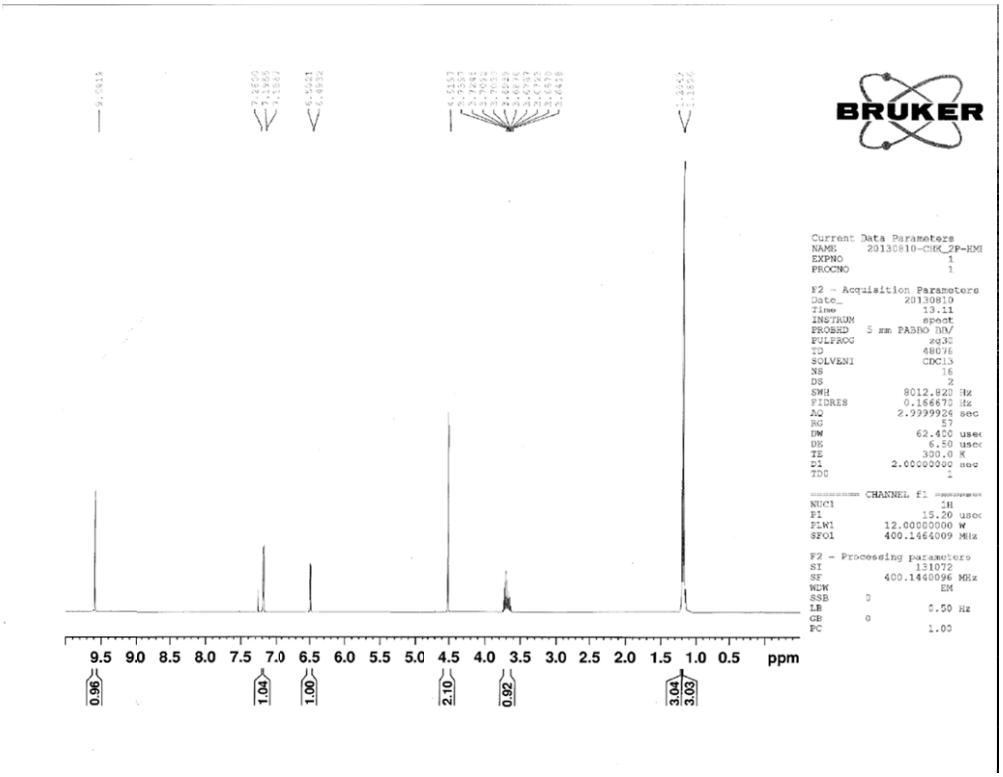

The ^{1}H spectrum of 5-(isopropoxymethyl)furan-2-carbaldehyde

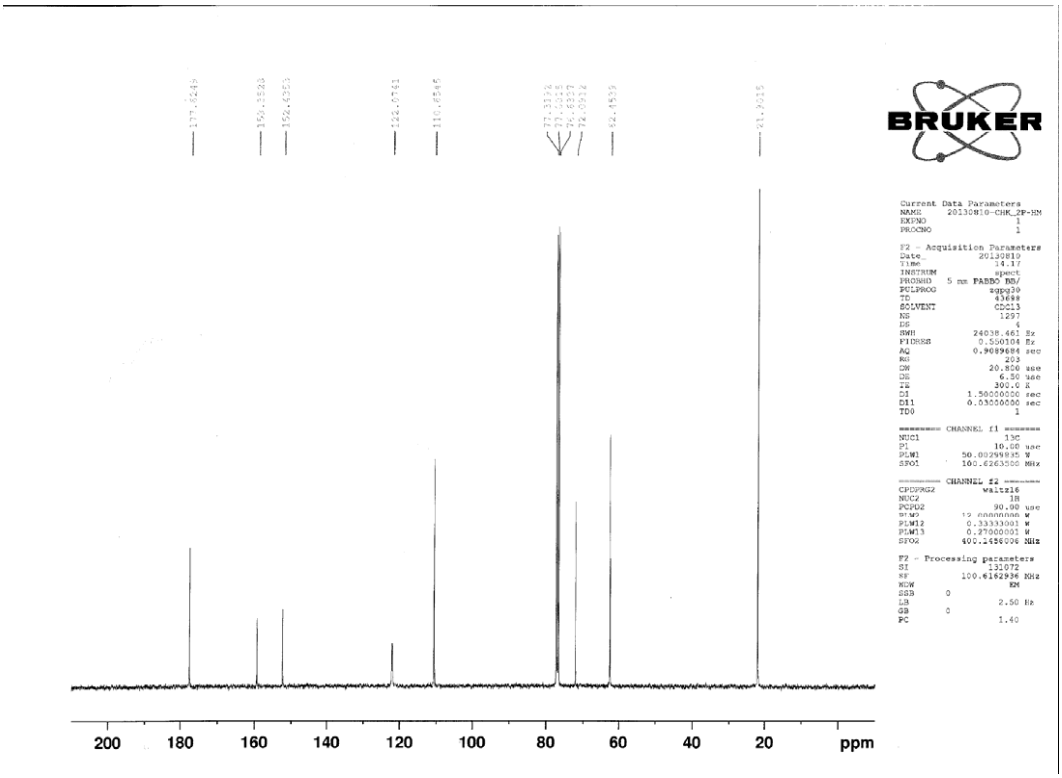

The ^{13}C spectrum of 5-(isopropoxymethyl)furan-2-carbaldehyde

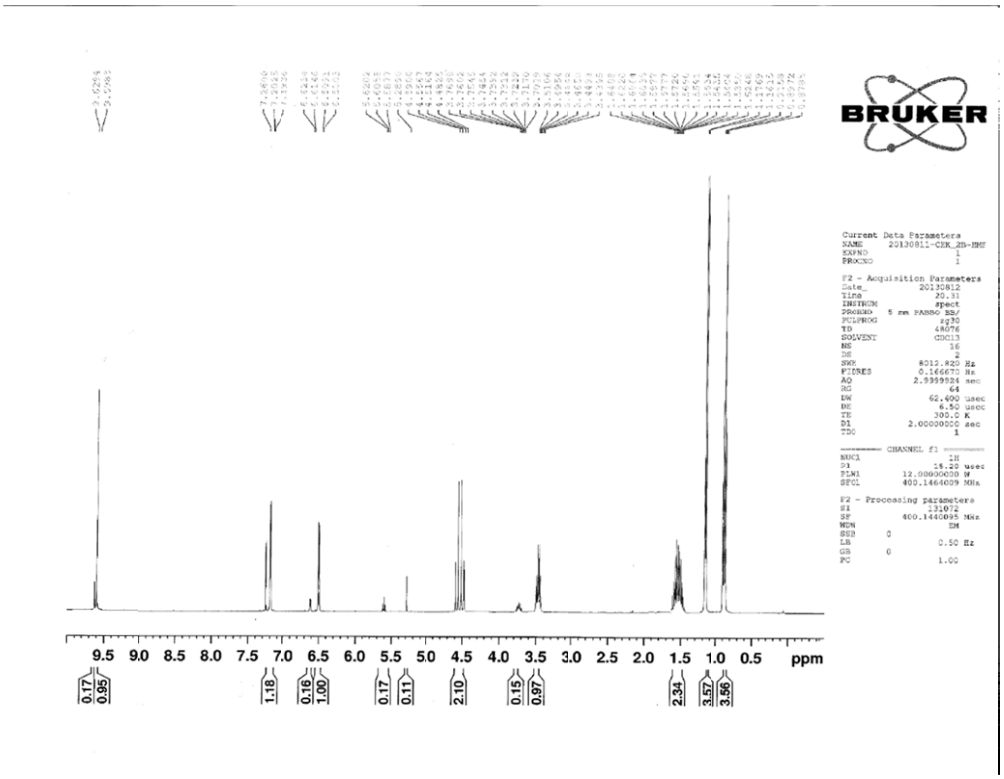

The ^{1}H spectrum of 5-(*sec*-butoxymethyl)furan-2-carbaldehyde

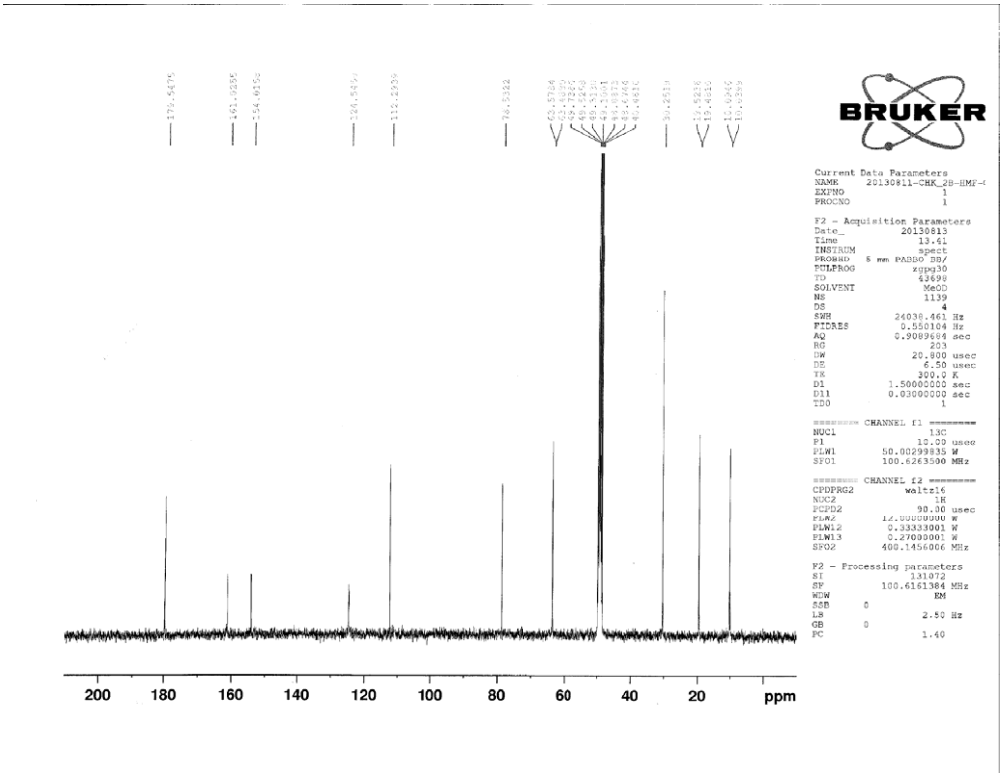

The ^{13}C spectrum of 5-(*sec*-butoxymethyl)furan-2-carbaldehyde

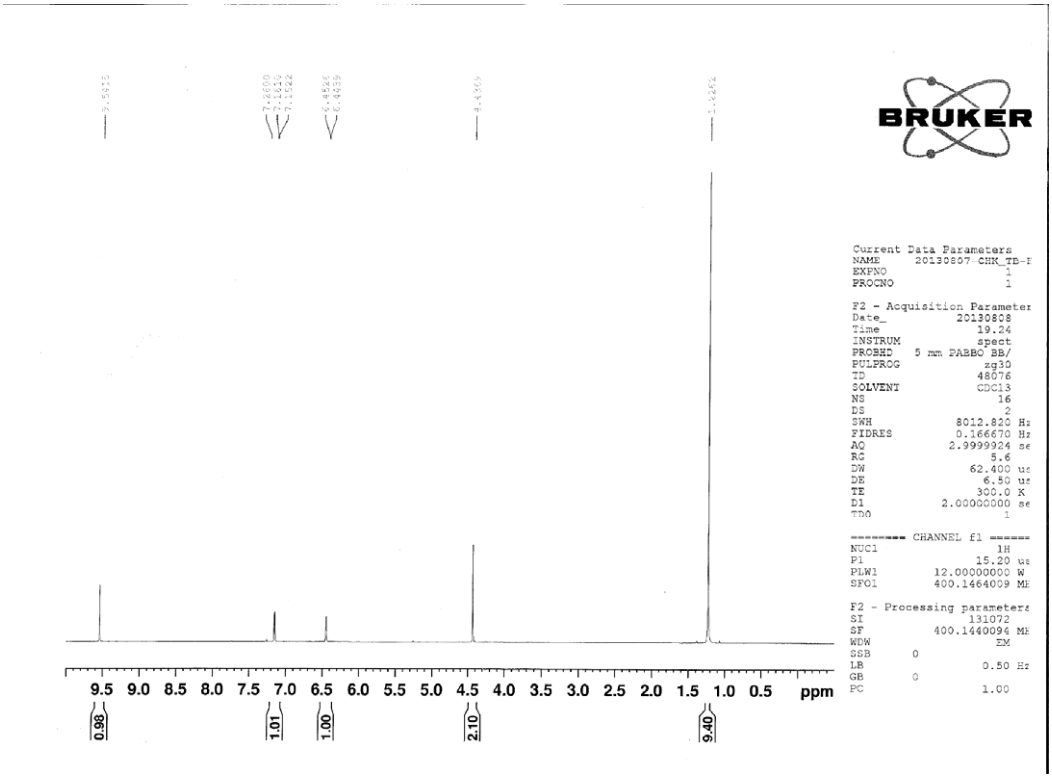

The ^{1}H spectrum of 5-(*tert*-butoxymethyl)furan-2-carbaldehyde

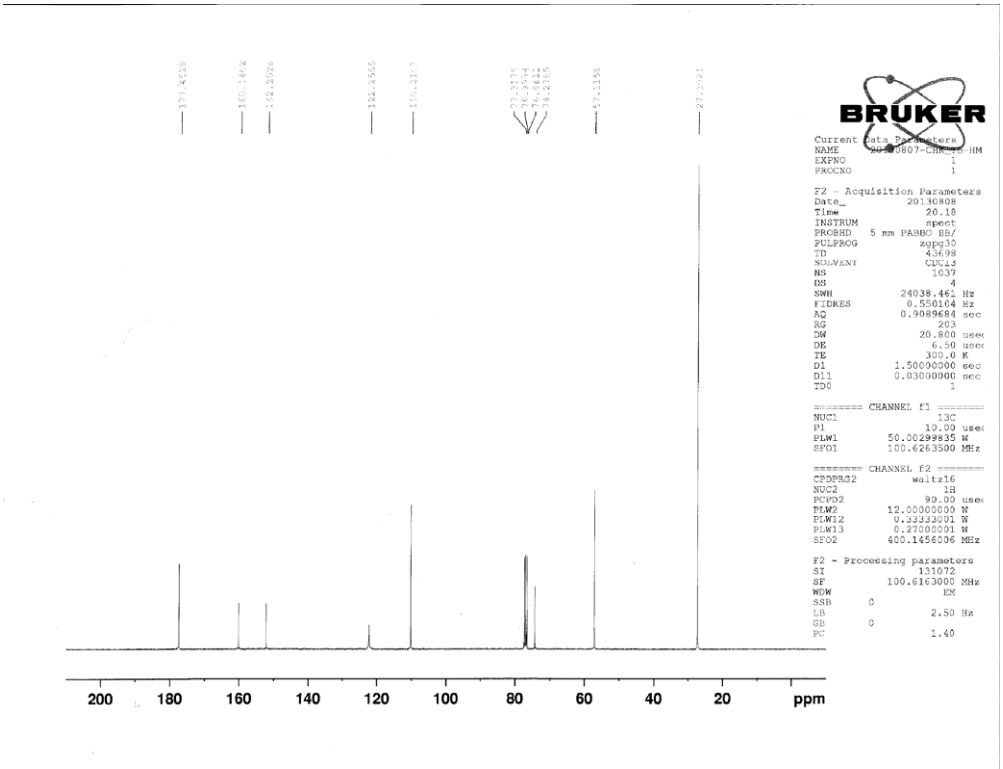

The ^{13}C spectrum of 5-(*tert*-butoxymethyl)furan-2-carbaldehyde